PHYSICAL REVIEW B **84**, 100402(R) (2011)

Lattice-driven magnetoresistivity and metal-insulator transition in single-layered iridates

M. Ge,[1,2,3] T. F. Qi,[1,2] O. B. Korneta,[1,2] D. E. De Long,[1,2] P. Schlottmann,[4] W. P. Crummett,[1,5] and G. Cao[1,2,*]

[1]*Center for Advanced Materials, University of Kentucky, Lexington, Kentucky 40506, USA*

[2]*Department of Physics and Astronomy, University of Kentucky, Lexington, Kentucky 40506, USA*

[3]*China High Magnetic Field Lab and University of Science and Technology of China, Hefei, China*

[4]*Department of Physics, Florida State University, Tallahassee, Florida 32306, USA*

[5]*Department of Physics, Centre College, Danville, Kentucky 40422, USA*

(Received 21 July 2011; revised manuscript received 15 August 2011; published 9 September 2011)

Sr_2IrO_4 exhibits an insulating state driven by spin-orbit interactions. We report two phenomena, namely, a large magnetoresistivity in Sr_2IrO_4 that is extremely sensitive to the orientation of magnetic field but exhibits no apparent correlation with the magnetization, and a robust metallic state that is induced by dilute electron (La^{3+}) or hole (K^+) doping for Sr^{2+} ions in Sr_2IrO_4. Our structural, transport, and magnetic data reveal that a strong spin-orbit interaction alters the balance between the competing energies so greatly that (1) the spin degree of freedom alone is no longer a dominant force, (2) the underlying transport properties delicately hinge on the Ir-O-Ir bond angle via a strong magnetoelastic coupling, and (3) a highly insulating state in Sr_2IrO_4 is proximate to a metallic state, and the transition is governed by lattice distortions that can be controlled via either the magnetic field or chemical doping.

DOI: 10.1103/PhysRevB.84.100402 PACS number(s): 75.47.De, 71.70.Ej, 75.47.Lx, 75.30.Gw

The 5*d*-based iridates have become a fertile ground for studies of physics driven by strong spin-orbit interactions; this physics is embodied by a large array of phenomena observed recently, such as the $J_{\rm eff} = 1/2$ Mott insulator,[1–3] a hyperkagome structure,[4] a giant magnetoelectric effect,[5] exotic metallic states,[6,7] unusual orbital magnetism,[8] etc. The list of relevant theoretical proposals is already long and intriguing: high T_c superconductivity,[9] correlated topological insulators,[10,11] Dirac semimetals with Fermi arcs,[12] the Kitaev mode,[12,13] etc. It is known that the relativistic spin-orbit interaction proportional to Z^4 (where Z is the atomic number) ranges from 0.2 to 1 eV in 5*d* materials (as compared to ∼20 meV in 3*d* materials), therefore, it can no longer be treated as a perturbation as is in many other materials where the magnetic interaction is dominated by the spin degree of freedom alone. Instead, the strong spin-orbit interaction vigorously competes with Coulomb (0.5–2 eV) and other interactions, and thus sets a balance between the relevant energies that drive exotic states that have been seldom or, to the best of knowledge, have never been seen in other materials; the findings reported here constitute an example.

Sr_2IrO_4, with a crystal structure similar to that of La_2CuO_4 and the *p*-wave superconductor Sr_2RuO_4, is a weak ferromagnet (FM) with a Curie temperature $T_C = 240$ K.[14–17] A unique and important structural feature of Sr_2IrO_4 is that it crystallizes in a reduced tetragonal structure (space group $I4_1/acd$) due to a rotation of the IrO_6 octahedra about the *c* axis by ∼11°, resulting in a larger unit cell by $\sqrt{2} \times \sqrt{2} \times 2$.[14–17] This rotation corresponds to a distorted in-plane Ir1-O2-Ir1 bond angle θ that is critical to the electronic structure.[7,9,12,18] It is already established that Sr_2IrO_4 is a unique Mott insulator dictated by spin-orbit interactions.[1–3] In essence, strong crystal fields split off 5*d* band states with e_g symmetry, and t_2g bands arise from $J_{\rm eff} = 1/2$ and $J_{\rm eff} = 3/2$ multiplets via a strong spin-orbit interaction (∼0.4 eV). A weak admixture of the e_g orbitals downshifts the $J_{\rm eff} = 3/2$ quadruplet from the $J_{\rm eff} = 1/2$ doublet. Since the Ir^{4+} ($5d^5$) ions provide five electrons, four of them fill the lower $J_{\rm eff} = 3/2$ bands, and one electron partially fills the $J_{\rm eff} = 1/2$ band. The $J_{\rm eff} = 1/2$ band is so narrow that even a reduced Coulomb repulsion U (∼0.5 eV) is sufficient to open a small gap that supports the insulating state.[1,2] A similar mechanism also describes insulating states observed in other iridates, such as $Sr_3Ir_2O_7$[2,19] and $BaIrO_3$.[8,20]

In this Rapid Communication, we report the following central findings for single-crystal Sr_2IrO_4 and its derivatives with dilute doping: (1) The magnetic structure varies with temperature *T*, resulting in three temperature regions that show distinct magnetotransport behavior; (2) the isothermal resistivity $\rho(H)$ exhibits a large, lattice-driven magnetoresistivity punctuated with multiple transitions that is highly sensitive to the orientation of the magnetic field *H*, but shows no apparent correlation with the isothermal magnetization $M(H)$ when $H \| c$ axis; and (3) a robust metallic state is readily induced by dilute doping of either La^{3+} or K^+ ions for Sr^{2+} ions in Sr_2IrO_4, highlighting the proximity of the insulating state to a metallic state that is mainly controlled by the lattice distortions. The findings point to a general conclusion that the underlying electronic properties are governed by lattice distortions or the Ir-O-Ir bond angle; and this work illustrates that the bond angle can be controlled through either a magnetic field or chemical doping. The spin degree of freedom alone is no longer a driving force due to the strong spin-orbit interaction. These phenomena open an alternate avenue for studies of physics driven by spin-orbit coupling, and also pose unique device paradigms for lattice-driven electronic materials.

The single crystals studied were synthesized using a self-flux technique described elsewhere.[5–7,16,19,20] The average size of the single crystals was $1.0 \times 0.7 \times 0.2$ cm^3. The structures of $(Sr_{1-x}La_x)_2IrO_4$ and $(Sr_{1-x}K_x)_2IrO_4$ were determined using a Nonius Kappa CCD x-ray diffractometer with the sample temperature controlled using a nitrogen stream. Structures were refined by full-matrix least squares using the SHELX-97 programs.[21] Chemical compositions of the single crystals were determined using energy-dispersive x-ray analysis (EDX).

Resistivity $\rho(T,H)$ and magnetization $M(T,H)$ were measured using a Quantum Design (QD) 7T superconduction quantum interference device (SQUID) magnetometer and a QD 14T physical property measurement system, respectively.

This study captures a few critical magnetic features of Sr_2IrO_4 that need to be addressed first. While both the a-axis $M_a(T)$ and the c-axis $M_c(T)$ expectedly show ferromagnetic (FM) order below $T_C = 240$ K and a positive Curie-Weiss temperature $\theta_{CW} = +236$ K, and confirm the FM exchange coupling at high T,[5,7,14–17] a close examination of the low-field $M(T)$ reveals two additional anomalies at $T_{M1}\approx 100$ K and $T_{M2}\approx 25$ K in $M_a(T)$ and $M_c(T)$ [see Fig. 1(a)]. Our previous ac magnetic susceptibility also exhibits a peak near T_{M1} as well as a frequency dependence that is indicative of magnetic frustration.[5] Indeed, a recent muon-spin rotation (μSR) study of Sr_2IrO_4 reports two structurally equivalent muon sites that experience increasingly distinct local magnetic fields for $T<100$ K, which subsequently lock in below 20 K.[22] It becomes clear that the magnetic structure varies with T, resulting in three well-defined temperature regions I, II, and III [Fig. 1(a)], which exhibit distinct physical properties, as discussed below. Moreover, $M_a(T)$ decreases rapidly below T_{M1} and T_{M2}, but $M_c(T)$ rises below 50 K and more sharply below T_{M2} as T decreases [see the Fig. 1(a) inset]. The different T dependences of $M_a(T)$ and $M_c(T)$ signal an evolving magnetic structure where the spins may no longer lie within the basal plane below T_{M1}. This spin reorientation apparently simultaneously weakens M_a but enhances M_c, thereby reducing the magnetic anisotropy M_a/M_c, which decreases from 2.2 at 100 K to 1.5 at 1.7 K [see Figs. 1(b) and 1(c)].

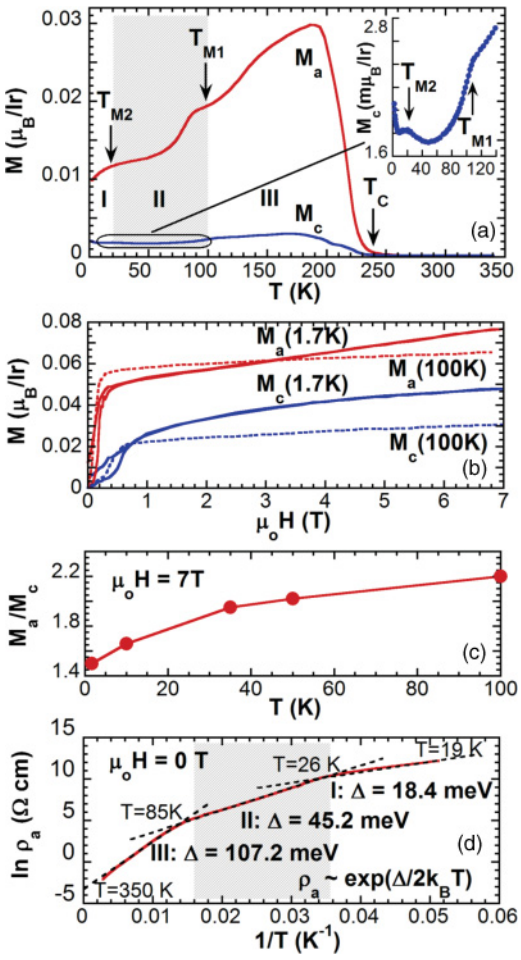

FIG. 1. (Color online) The field-cooled magnetization for the a axis and the c axis, M_a and M_c, as a function of (a) temperature at $\mu_o H = 0.1$ T, and (b) magnetic field at $T = 1.7$ and 100 K. (c) The magnetic anisotropy M_a/M_c as a function of temperature. (d) The resistivity for the a-axis $\ln \rho_a$ as a function of $1/T$. Inset in (a): Enlarged low-T M_c. Note that the data in (a) and (d) define regions I, II, and III.

The electrical resistivity for the a-axis $\rho_a(T)$ follows an activation law $\rho_a(T)\sim\exp(\Delta/2k_BT)$ (where Δ is the energy gap and K_B is Boltzmann's constant), and exhibits three distinct values of Δ in regions that closely correspond to regions I, II, and III defined above, as shown in Fig. 1(d). It is noteworthy that Δ in region III is quite close to the optically measured gap ($\sim$0.1 eV);[1] and it further narrows with decreasing T [Fig. 1(d)] and, unexpectedly, with the application of a modest magnetic field of a few Tesla (not shown).

Indeed, the transport properties are coupled to H in such a peculiar fashion that, to the best of our knowledge, no current models can describe the observed magnetoresistivity shown in Figs. 2 and 3. We focus on a representative temperature $T = 35$ K that is within region II. For the $H\|a$ axis, both the a-axis resistivity $\rho_a(H\|a)$ [Fig. 2(b)] and the c-axis resistivity $\rho_c(H\|a)$ [Fig. 2(c)] exhibit an abrupt drop by $\sim$60% near $\mu_o H = 0.3$ T, where a metamagnetic transition occurs, suggesting a spin reorientation, consistent with early studies.[5,16] These data partially track the field dependences of $M_a(H)$ and $M_c(H)$ shown in Fig. 2(a), suggesting a reduction of spin scattering;[23] but given the ordered moment $m_s<0.07\mu_B$/Ir, the reduction of spin scattering alone certainly cannot account for such a drastic reduction in $\rho(H)$. Even more strikingly, for the $H\|c$ axis, both $\rho_a(H\|c)$ and $\rho_c(H\|c)$ exhibit multiple anomalies at $\mu_o H = 2$ and 3 T, which leads to a large overall resistivity reduction of more than 50%; however, no anomalies corresponding to these transitions in $M_a(H)$ and $M_c(H)$ are discerned. (In addition, dM/dH shows no slope change near $\mu_o H = 2$ and 3 T.) Such behavior is clearly not due to the Lorenz force because $\rho_c(H\|c)$ exhibits the same behavior in a configuration where both the current and H are parallel to the c axis [Fig. 2(c)]; the conspicuous lack of the correlation between ρ and M is, to the best of our knowledge, apparently not endorsed by any existing models describing magnetoresistivity observed in other known materials.

An essential contributor to conventional magnetoresistance is spin-dependent scattering; negative magnetoresistance can be a result of the reduction of spin scattering due to spin alignment with increasing magnetic field. The data in Fig. 2 therefore raise a fundamental question: Why does the resistivity sensitively depend on the orientation of magnetic field H but shows no direct relevance to the measured magnetization when H is parallel to the c-axis? While we are not aware of any conclusive answers to the question, one scenario may be qualitatively relevant.

This scenario is based on the following understanding established in this and in previous work on Sr_2IrO_4: (1) In the case of strong spin-orbit interaction, the lattice distortion, or specifically, the Ir1-O2-Ir1 bond angle θ, dictates the low-

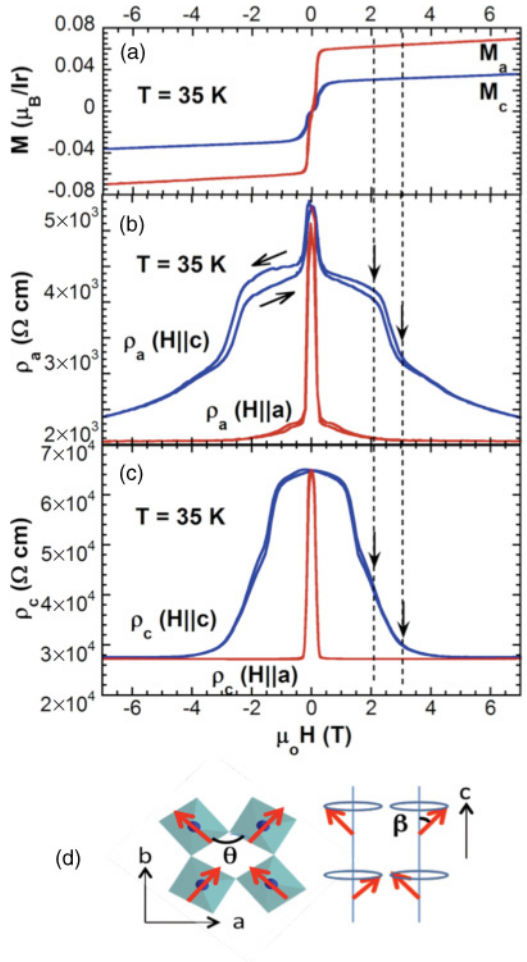

FIG. 2. (Color online) The field dependence at $T = 35$ K of (a) the magnetization M_a and M_c. (b) The a-axis resistivity ρ_a for $H\|a$ and $H\|c$. (c) The c-axis resistivity ρ_c for $H\|a$ and $H\|c$. (d) The schematics of the spin configuration for the basal plane (left-hand side) and the ac plane (right-hand side).

energy Hamiltonian[12] and the band structure.[7,18] (2) A strong spin-orbit interaction can cause the spins to rigidly rotate with the IrO_6 octahedra via strong spin-lattice or magnetoelastic coupling.[5,12] (3) The reduced magnetic anisotropy M_a/M_c strongly indicates an emerging c-axis spin component below T_{M1} that generates a noncollinear spin structure and frustration, as manifested in Fig. 1, and in previous studies;[5,12,22] the noncollinearity could take the form of a spiral spin configuration where the spin direction is rigidly maintained at an angle β with respect to the c axis, as sketched in Fig. 2(d).

Recent studies of Sr_2IrO_4 have already established that electron hopping sensitively depends on the bond angle θ.[7] In particular, hopping occurs through two active t_{2g} orbitals: d_{xy} and d_{xz} for θ=180°, and d_{xz} and d_{yz} for θ=90°.[12] It is recognized that the larger the θ, the more energetically favorable it is for electron hopping and superexchange interactions. Since the IrO_6 octahdra rotate with the spins, the application of the $H\|c$ axis must at least slightly rotate the IrO_6 octahdra about the c axis, which, in turn, changes θ. It is important to realize that even a small increase in θ due to increasing H can be sufficient to drastically enhance the hopping, which could explain the multiple downturns in $\rho(H)$. The clear hysteresis exhibited in Fig. 2(b) reinforces the notion that the magnetoresistivity is primarily driven by field-induced lattice distortions for $H\|c$. The absence of anomalies in $M_a(H)$ and $M_c(H)$ corresponding to the transitions in $\rho_a(H)$ and $\rho_c(H)$ can be attributed to a spiral spin configuration: The spins respond to H only by rotating about the c axis, and this rotation changes θ but does not affect β or the c- and a-axis projection of the magnetic moment, as schematically illustrated in Fig. 2(d); therefore, $M_a(H)$ and $M_c(H)$ remain unchanged, at least up to $\mu_o H = 14$ T, the highest field available in our laboratory. Such behavior may be retained at even higher H given the nearly saturated $M_a(H)$ and $M_c(H)$ at 14 T (not shown).

The delicate nature of the coupling of the magnetotransport behavior to the lattice and magnetic structure is apparent in a few respects, as illustrated in Fig. 3. The transport behavior seen in region II is no longer observable in region I, where the magnetoresistivity is extremely weak; this is evident in $\rho_a(H)$ and $\rho_c(H)$ at $T = 10$ K, as shown in Fig. 3(a). Moreover, the application of the $H\|a$ axis causes a pronounced rise in $\rho_a(H)$ rather than the sharp drop observed in region II at low H [Figs. 2, 3(b), and 3(c)], and a reversal of the resistivity anisotropy [Fig. 3(a)]. On the other hand, as T approaches region III, the field dependence of $\rho_a(H)$ and $\rho_c(H)$ retains some resemblance to that in region II, but it becomes far weaker.

Indeed, the electronic state can be readily changed via slight manipulations of θ, and θ can be controlled through either the magnetic field, as illustrated in Figs. 2 and 3, or chemical doping. As documented in Fig. 4(a), a dilute doping of either La^{3+} or K^{+} ions for Sr^{2+} ions leads to a

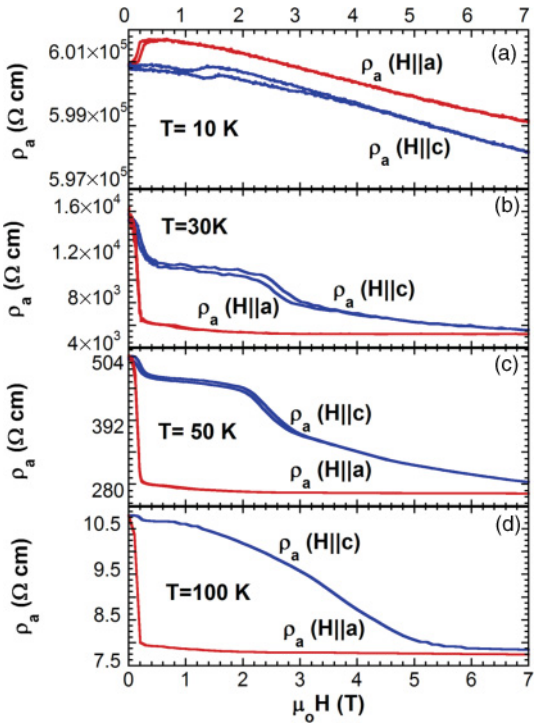

FIG. 3. (Color online) The field dependence of the a-axis resistivity ρ_a for $H\|a$ and $H\|c$ at representative temperatures at (a) $T = 10$ K (region I), (b) $T = 30$ K, (c) $T = 50$ K, and (d) $T = 100$ K (approaching region III).

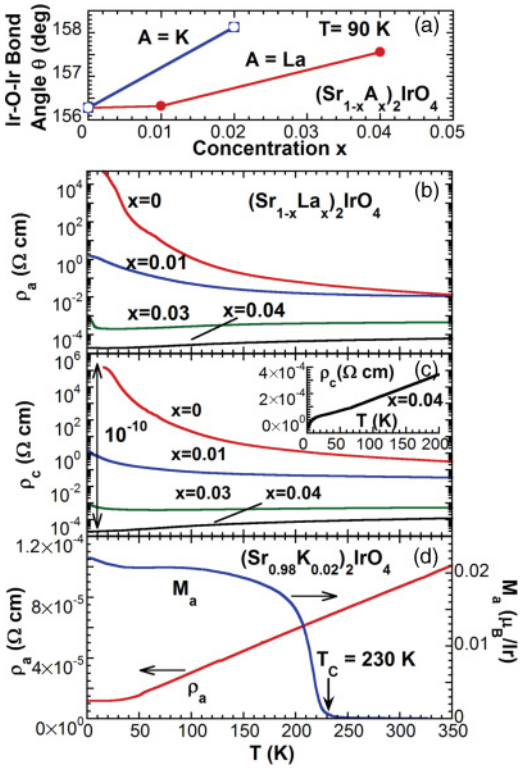

FIG. 4. (Color online) (a) The Ir1-O2-Ir1 bond angle θ as a function of La and K doping concentration x. The temperature dependence of (b) the a-axis resistivity ρ_a, and (c) the c-axis resistivity ρ_c for $(Sr_{1-x}La_x)_2IrO_4$ with $0 \leqslant x \leqslant 0.04$; (d) The temperature dependence of ρ_a and M_a at $\mu_o H = 0.1$ T (right-hand scale) for $(Sr_{0.98}K_{0.02})_2IrO_4$. Inset in (c): Enlarged low-T ρ_c.

larger θ despite considerable differences between the ionic radii of Sr, La, and K, which are 1.18, 1.03, and 1.38 Å, respectively. Since hopping between active t_2g orbitals is critically linked to θ, drastic changes in physical properties due to such sizable increases in θ are anticipated. It is therefore understandable that ρ_a (ρ_c) is reduced by a factor of 10^{-8} (10^{-10}) at low T as x evolves from 0 to 0.04 and 0.02 for La and K, respectively [see Figs. 4(b)–4(d)]. For a La doping of $x = 0.04$, there is a sharp downturn near 10 K, indicative of a rapid decrease in inelastic scattering [Fig. 4(c) inset]. Such low-T behavior is similar to that observed in slightly oxygen-depleted $Sr_2IrO_{4-\delta}$ with $\delta = 0.04$.[7] It is noteworthy that T_C decreases with La doping in $(Sr_{1-x}La_x)_2IrO_4$ (not shown), and vanishes at $x = 0.04$ where the metallic state is fully established (an early study[24] also shows a decrease in resistivity in 2.5% of La-doped polycrystalline Sr_2IrO_4); in contrast, the magnetically ordered state coexists with the fully metallic state in $(Sr_{0.98}K_{0.02})_2IrO_4$, as shown in Fig. 4(d). This comparison stresses that the occurrence of a metallic state does not necessarily accompany radical changes in the magnetic state in iridates; this observation is in accord with a conspicuous characteristic of Sr_2IrO_4 where the resistivity shows no anomaly near T_C (=240 K).[5,7,16] The radical changes in transport properties of Sr_2IrO_4 with dilute doping strongly suggest that the insulating state driven by a strong spin-orbit interaction is proximate to a metallic state. The induction of a robust metallic state by either dilute electron (La^{3+}) or hole (K^+) doping for Sr^{2+} further reinforces the central finding of this Rapid Communication that transport properties in iridates such as Sr_2IrO_4 can be chiefly dictated by the lattice degrees of freedom.

In summary, the large and uniquely anisotropic magnetoresistivity in Sr_2IrO_4 and the robust metallic state in doped Sr_2IrO_4 are attributed to the subtle unbuckling of the IrO_6 octahedra, without apparent correlation with the magnetization as conventionally anticipated; furthermore, the lattice distortions that dictate the underlying electronic properties in Sr_2IrO_4 can be controlled via either magnetic field or chemical doping. We conclude that a strong spin-orbit interaction fundamentally changes the balance between the competing energies such that (1) the spin degree of freedom alone is no longer a dominant variable, (2) electron hopping delicately depends upon the lattice distortion via strong magnetoelastic coupling, and (3) the highly insulating state in Sr_2IrO_4 is proximate to a metallic state. We expect such a unique magnetotransport behavior to result in different technological paradigms based upon lattice-driven electronic materials.

One of us (G.C.) is very thankful to G. Murphy and R. Kaul for enlightening discussions. This work was supported by NSF through Grants No. DMR-0856234 (G.C.) and No. EPS-0814194 (G.C., L.E.D.), and by DOE through Grants No. DE-FG02-97ER45653 (L.E.D.) and No. DE-FG02-98ER45707 (P.S.).

*Corresponding author: cao@uky.edu

[1] B. J. Kim, Hosub Jin, S. J. Moon, J.-Y. Kim, B.-G. Park, C. S. Leem, Jaejun Yu, T. W. Noh, C. Kim, S.-J. Oh, J.-H. Park, V. Durairai, G. Cao, and E. Rotenberg, Phys. Rev. Lett. **101**, 076402 (2008).

[2] S. J. Moon, H. Jin, K. W. Kim, W. S. Choi, Y. S. Lee, J. Yu, G. Cao, A. Sumi, H. Funakubo, C. Bernhard, and T. W. Noh, Phys. Rev. Lett. **101**, 226402 (2008).

[3] B. J. Kim, H. Ohsumi, T. Komesu, S. Sakai, T. Morita, H. Takagi, and T. Arima, Science **323**, 1329 (2009).

[4] Y. Okamoto, M. Nohara, H. Aruga-Katori, and H. Takagi, Phys. Rev. Lett. **99**, 137207 (2007).

[5] S. Chikara, O. Korneta, W. P. Crummett, L. E. DeLong, P. Schlottmann, and G. Cao, Phys. Rev. B **80**, 140407(R) (2009).

[6] G. Cao, V. Duarairaj, S. Chikara, L. E. DeLong, S. Parkin, and P. Schlottmann, Phys. Rev. B **76**, 100402(R) (2007).

[7] O. B. Korneta, Tongfei Qi, S. Chikara, S. Parkin, L. E. De Long, P. Schlottmann, and G. Cao, Phys. Rev. B **82** 115117 (2010).

[8] M. A. Laguna-Marco, D. Haskel, N. Souza-Neto, J. C. Lang, V. V. Krishnamurthy, S. Chikara, G. Cao, and Michel van Veenendaal, Phys. Rev. Lett. **105**, 216407 (2010).

[9] Fa Wang and T. Senthil, Phys. Rev. Lett. **106**, 136402 (2011).

[10] A. Shitade, H. Katsura, J. Kunes, X.-L. Qi, S.-C. Zhang, and N. Nagaosa, Phys. Rev. Lett. **102**, 256403 (2009).

[11] D. A. Pesin and Leon Balents, Nat. Phys. **6**, 376 (2010).

[12] G. Jackeli and G. Khaliulin, Phys. Rev. Lett. **102** 017205 (2009).

[13] Xiangang Wan, A. M. Turner, A. Vishwanath, and S. Y. Savrasov, Phys. Rev. B **83**, 205101 (2010).

[14]Q. Huang, J. L. Soubeyroux, O. Chmaissen, I. Natali Sora, A. Santoro, R. J. Cava, J. J. Krajewski, and W. F. Peck, Jr., J. Solid State Chem. **112**, 355 (1994).

[15]R. J. Cava, B. Batlogg, K. Kiyono, H. Takagi, J. J. Krajewski, W. F. Peck, Jr., L. W. Rupp, Jr., and C. H. Chen, Phys. Rev. B **49**, 11890 (1994).

[16]G. Cao, J. Bolivar, S. McCall, J. E. Crow, and R. P. Guertin, Phys. Rev. B **57**, R11039 (1998).

[17]M. K. Crawford, M. A. Subramanian, and R. L. Harlow, J. A. Fernandez-Baca, Z. R. Wang, and D. C. Johnston, Phys. Rev. B **49**, 9198 (1994).

[18]S. J. Moon, Hosub Jin, W. S. Choi, J. S. Lee, S. S. A. Seo, J. Yu, G. Cao, T. W. Noh, and Y. S. Lee, Phys. Rev. B **80**, 195110 (2009).

[19]G. Cao, Y. Xin, C. S. Alexander, J. E Crow, P. Schlottmann, M. K. Crawford, R. L. Harlow, and W. Marshall, Phys. Rev. B **66**, 214412 (2002).

[20]G. Cao, J. E. Crow, R. P. Guertin, P. F. Henning, C. C. Homes, M. Strongin, D. N. Basov, and E. Lochner, Solid State Commun. **113**, 657 (2000).

[21]G. M. Sheldrick, Acta Crystallogr A **64**, 112 (2008).

[22]I. Franke, P. J. Baker, S. J. Blundell, T. Lancaster, W. Hayes, F. L. Pratt, and G. Cao, Phys. Rev. B **83** 094416 (2011).

[23]Shuai Jiang, Yongkang Luo, Zhi Ren, Zengwei Zhu, Cao Wang, Xiangfan Xu, Qian Tao, Guanghan Cao, and Zhu'an Xu, New Journal of Physics **11** 025007 (2009).

[24]Y. Klein and I. Terasaki, J. Phys.: Condensed Mattter **20**, 295201 (2008).